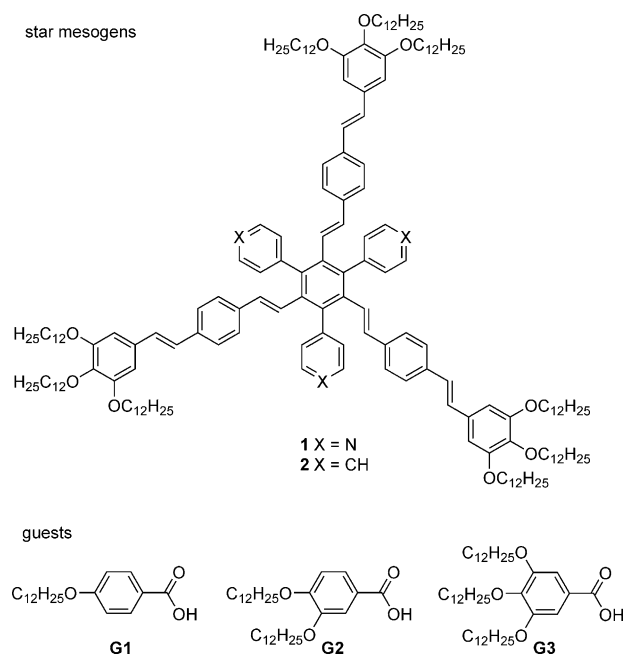


# Shape-Persistent, Sterically Crowded Star Mesogens: From Exceptional Columnar Dimer Stacks to Supermesogens\*\*

Matthias Lehmann\* and Philipp Maier

**Abstract:** Hexasubstituted  $C_3$ -symmetric benzenes with three oligophenylenevinylene (OPV) arms and three pyridyl or phenyl substituents are shape-persistent star mesogens that are sterically crowded in the center. Such molecular structures possess large void spaces between their arms, which have to be filled in condensed phases. For the neat materials, this is accomplished by an exceptional formation of dimers and short-range helical packing in columnar mesophases. The mesophase is thermodynamically stable for the pyridyl compound. Only this derivative forms filled star-shaped supermesogens in the presence of various carboxylic acids. The latter do not arrange as dimers, but as monomers along the columnar stacks. In this liquid crystal (LC) phase, the guests are completely enclosed by the hosts. Therefore, the host can be regarded as a new LC endoreceptor, which allows the design of columnar functional structures in the future.

The self-organization of non-conventional mesogens is a highly topical field of research, which has unraveled a large number of complex packing arrangements and thus contributed to gain structural control in functional materials. Bolaamphiphiles, shape-persistent macrocycles, and star-shaped mesogens belong to this class of extraordinary mesogens.<sup>[1–3]</sup> The latter formally possess large void spaces between their arms, which they compensate during the packing in condensed phases by folding processes to *E*- and cone-shaped conformers, and thus form a multitude of columnar and cubic phases.<sup>[3,4]</sup> Recently, we successfully showed that even shape-persistent star-shaped mesogens stack extremely dense in columnar phases; guests that were covalently bound within the free space between the arms stabilized the liquid crystal (LC) phases enormously and formed nanosegregated donor–acceptor aggregates.<sup>[5]</sup> We pursued a completely different approach with the title compounds **1** and **2** (Figure 1). With these sterically crowded, hexasubstituted benzene derivatives, we aimed to incorporate guest molecules through supramolecular interactions and thus to generate new functional materials. Although hydrogen bonding has been used to produce supermesogens for a long time,<sup>[6]</sup> the great majority of these systems consist of non-mesogenic core building blocks that bind the guests to their



**Figure 1.** Sterically crowded, shape-persistent star mesogens and their guests.

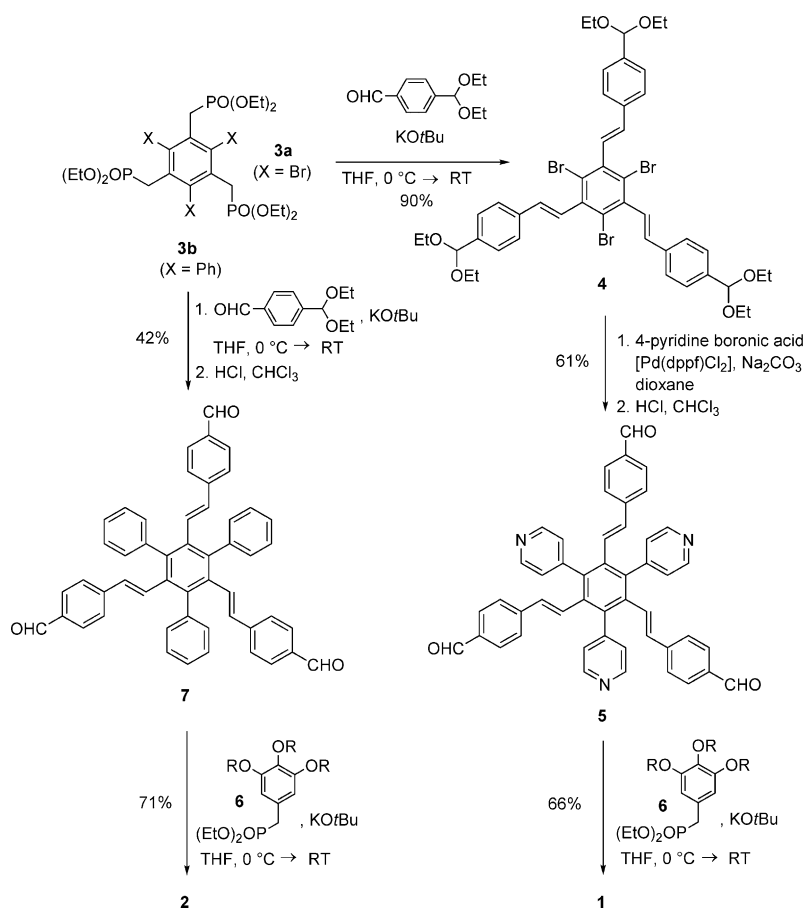
periphery as exoreceptors.<sup>[7]</sup> Only investigations by Janietz and Serrano have highlighted LC melamine derivatives that may host one guest at most, and consequently, they can be regarded as endoreceptors.<sup>[8]</sup> LC materials from hexasubstituted benzene derivatives are rarely observed when the arms consist of shape-persistent conjugated arms.<sup>[9]</sup> For such star compounds, where the lengths of the arms are greater than the size of a phenyl group, LC phases have been disclosed.<sup>[10,11]</sup>

The target compounds **1** and **2** are  $C_3$ -symmetric mesogens, in which every second arm is elongated to generate the cavities of the star molecules. Herein, we show that the new star molecules reveal LC phases despite their sterically crowded core. In this mesogen family, the filling of the voids proceeds through the exceptional formation of dimers in the phases of the neat compounds, which is confirmed by X-ray scattering, fiber pattern simulation, and modelling. The dimers consisting of two mesogens **1** are obviously stabilized by dipole–dipole interactions of the pyridyl units oriented in an antiparallel fashion, as confirmed by the formation of an enantiotropic mesophase for compound **1**, whereas compound **2** forms only a monotropic mesophase at low temperature. Mixtures with different guests **G1–G3** result in new stable LCs exclusively for acceptor mesogen **1**.

[\*] Prof. Dr. M. Lehmann, P. Maier  
Institut of Organic Chemistry, University of Würzburg  
Am Hubland, 97074 Würzburg (Germany)  
E-mail: Matthias.Lehmann@uni-wuerzburg.de

[\*\*] We thank the German Science Foundation (DFG, LE 1571-5.1) for financial support.

Supporting information for this article is available on the WWW under <http://dx.doi.org/10.1002/anie.201501988>.



**Scheme 1.** Synthesis of the target compounds **1** and **2** (R = C<sub>12</sub>H<sub>25</sub>).

The combination of a threefold Wittig–Horner reaction with a threefold Suzuki coupling leads to the synthesis of the hexasubstituted target compounds **1** and **2** (Scheme 1). The synthesis of molecule **1** started with the conversion of the trisphosphonate **3a** into trisacetal **4** in a Wittig–Horner reaction. Subsequent Suzuki coupling of the pyridylboronic acid and hydrolysis of the acetals furnished the trisaldehyde **5** in 61% yield. The final Wittig–Horner reaction with phosphonate **6** afforded the desired product. The inversion of the first two steps—first the incorporation of the phenyl groups, then the Wittig–Horner reaction to afford the trisacetal—appeared to be optimal for the preparation of compound **2**. The isolation of the materials is demanding, as molecules with less than six arms have to be separated, a task that has already been shown to be challenging for different hexasubstituted compounds in the past.<sup>[12]</sup> The purity of the materials was demonstrated by standard methods (NMR, elemental analysis, and mass spectrometry). Characteristic for such compounds **1** and **2** is the enormous high field shift of the doublets attributed to the protons of the inner double bonds from  $\delta = 7.14/7.20$  ppm for the parent compound with only three OPV arms<sup>[5b]</sup> to  $\delta = 6.4$  (6.5) and 5.8 (5.8) ppm. This shift is caused by the anisotropy effect of the neighboring aromatic building blocks (see the Supporting Information).

The thermotropic properties of the star-shaped compounds **1** and **2** as well as selected mixtures with guests **G1**–**G3** were investigated by means of polarized optical micros-

copy (POM), differential scanning calorimetry (DSC), and X-ray scattering and are summarized in Table 1. Both stars **1** and **2** form a hexagonal columnar LC phase, which was confirmed by characteristic pseudo-focal conic textures and the reciprocal spacing of the reflections in the ratio of  $d_{100}^{-1}/d_{110}^{-1}/d_{200}^{-1} = 1:\sqrt{3}:2$  (Figure 2). The shearability of the samples, the absence of reflections at wide angles, and the halo with a maximum at 4.6 Å (**1**) or 4.8 Å (**2**)—values that are attributed to the average separation of the disordered alkyl chains—confirm the LC nature of these phases. The rather small structural differences at the inner aromatic rings of compounds **1** and **2** lead to completely different phase stabilities. Whereas **2** with phenyl rings at the center forms only a monotropic mesophase at low temperature (clearing temperature  $T_{Cl} = 34$  °C), the dipole moments of the pyridyl groups in **1** obviously stabilize the aggregation in the columnar phase, which results in an enantiotropic Col<sub>h</sub> phase with a  $T_{Cl}$  that is more than 100 °C higher ( $T_{Cl} = 139$  °C).

To understand the self-assembly of these exceptional mesogens, the number of molecules  $Z$  in a columnar repeating unit was first calculated with  $Z = \rho N_A V/M$  assuming a density of  $\rho = 1$  g cm<sup>-3</sup>. The volume  $V$  was determined according to  $V = a^2 c \sin 60^\circ$  (height  $c = 4.6$  and 4.8 Å for **1** and **2**; respectively). Two

**Table 1:** Thermotropic properties of the stars and their mixtures.

No.	$T_{\text{transition}}$ (Onset) [°C]/ $\Delta H$ [kJ mol <sup>-1</sup> ] <sup>[a]</sup>	$a^{[b]}$ [Å] ( $T$ [°C])	$d_{\text{halo}}$ [Å]	$c^{[c]}$ [Å]	$Z^{[c]}$
<b>1</b>	Col <sub>hg</sub> 85 (T <sub>g</sub> ) Col <sub>h</sub> 139/5.7 I	46.7 (93)	4.5	4.6	2.0
<b>2</b>	Cr 55/47.8 (Col <sub>h</sub> 34/0.8) I	44.8 (23)	4.8	4.8	2.0
<b>1G1<sub>11</sub></b>	Col <sub>h</sub> 144/6.3 I	45.4 (93)	4.5	5.4	2.0
<b>1G1<sub>12</sub></b>	Cr 60/12.6 Col <sub>h</sub> 143/5.8 I	45.3 (93)	4.5	6.0	2.0
<b>1G1<sub>13</sub></b>	Cr 71/103.2 Col <sub>h</sub> 136/6.8 I	45.0 (93)	4.5	3.3	1.0
<b>1G2<sub>13</sub></b>	Cr 95/56.6 Col <sub>h</sub> 124/2.8 I	44.5 (101)	4.6	3.9	1.0
<b>1G3<sub>13</sub></b>	Col <sub>h</sub> 89/6.0 I	44.0 (93)	4.6	4.6	1.0

[a] Data of the second or third heating cycle of the DSC; Cr = crystal, Col<sub>h</sub> = columnar hexagonal phase, Col<sub>hg</sub> = glassy columnar hexagonal phase, I = isotropic phase. **1GX** (X = 1–3): mixture between **1** and guest **GX**, index (11, 12, 13): ratio (1:1, 1:2, 1:3) between host **1** and guest **GX**.

[b]  $a$  = unit cell parameter (diameter of the column). [c]  $c$  = height of the columnar unit filled by  $Z$  molecules at a density of 1 g cm<sup>-3</sup> ( $c = MZ/(\rho N_A A)$ ;  $M$  = molar mass,  $\rho$  = density,  $N_A$  = Avogadro's constant,  $A$  = area of the unit cell ( $A = a^2 \sin 60^\circ$ ); for **1**, the minimal density was determined to be 0.98 g cm<sup>-3</sup> at 22 °C by means of the buoyancy method (see the Supporting Information).

molecules occupy such a columnar section with the height  $c$  (Table 1). The mesogens cannot stack on top of each other in such a small columnar height as they are shape-persistent and sterically crowded in the center. A feasible solution is the formation of a dimer with two interdigitated mesogens

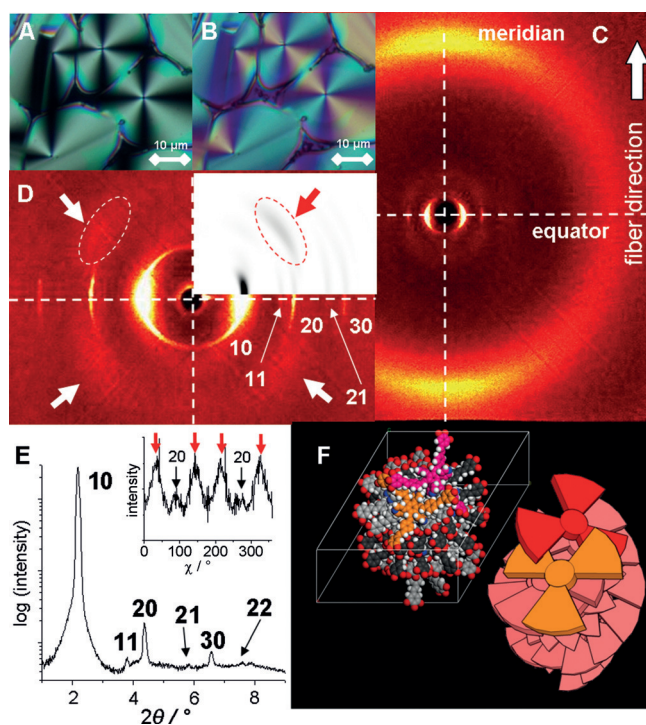


**Figure 2.** POM textures of **1** at 125 °C A) without and B) with a  $\lambda$ -compensation plate in the  $\text{Col}_h$  phase. C) WAXS and D) MAXS of an oriented sample **1** at 93 °C. The inset highlights the simulation (Program Clearer) based on the helical model (F). E) Integration of the diffraction pattern along the equator and  $\chi$ -scan of the set of four diffuse signals from D (inset, bold arrows). F) Model of the helically stacked dimers (Materials Studio) and schematic representation of the self-organization of the dimers; the aliphatic chains are not shown for clarity.

(Figure 2F). In such an aggregate, the dipoles of two pyridyl groups of **1** are oriented in an antiparallel arrangement and thus contribute to the stability. This stabilization is missing for compound **2**. To obtain more detailed information on the packing behavior, oriented fibers of **1** were studied comprehensively by X-ray scattering techniques (wide- (WAXS) and middle-angle X-ray scattering (MAXS); Figure 2C,D). The intense equatorial reflections attest the good orientation of the columnar phase. The higher intensity of the halo at the meridian confirms that the mesogens are on average oriented orthogonally to the column axes with a mean hydrocarbon separation of 4.6 Å. Furthermore, a set of four diffuse signals is observed left and right of the meridian and above and below the 20 reflections. A  $\chi$ -scan discloses that the intensity of these hardly visible signals is even higher than that of the 20 reflections. These diffuse reflections are positioned at a layer line, which corresponds to a periodicity of 32.1 Å along the column direction. Precisely seven dimers can occupy a columnar unit of this dimension. Stacks of such a large periodicity with the mesogens orthogonal to the columnar axis can be accomplished only by helical self-assembly. Owing to the symmetry of the dimers, a double helix is formed, and periodicity is achieved already after half of the helical pitch. Therefore, the full helical pitch amounts to 64.2 Å. However, reflections corresponding to this distance are not observed as

the reflections of the first layer line are systematically absent for a double helix.<sup>[13]</sup> Consequently, the very diffuse signals are located at the second layer line. The width of the reflections points to a small correlation length of the helical packing. A model of the columnar hexagonal phase was obtained with the program package Materials Studio and geometry-optimized (Figure 2F). The subsequent simulation of the fiber diffraction pattern with the program Clearer<sup>[14]</sup> furnished a simulated diffraction pattern (Figure 2D, inset) that is in very good agreement with the experimental data. This result confirms our model, in which the shape-persistent, star-shaped mesogens compensate the voids between their arms by the formation of dimers and their helical packing along the columns.

Guest molecules should also be able to occupy the interspaces of the stars and generate stable mesophases. The pyridyl building blocks bind the carboxylic acids by hydrogen bonding between the arms. The results of mixing star mesogen **1** with guest **G1** are shown in Figure 3. With an increase in the

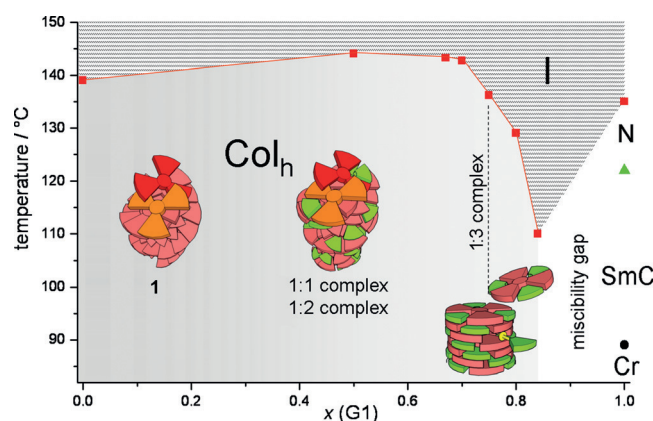


**Figure 3.** Phase diagram of mixtures of mesogen **1** with guest **G1** (transition temperatures (Onset/°C, DSC) versus the molar ratio of guest **G1**). Thermotropic properties of the guest **G1** ( $x=1$ ): Cr 89 °C SmC 122 °C N 135 °C I;<sup>[15]</sup> Cr = crystal, SmC = smectic C, N = nematic phase.

molar ratio of the guest  $x(\text{G1})$ , the clearing temperature first increases by 5 °C (host/guest = 1:1;  $x=0.5$ ); it subsequently drops by 1 °C for the 1:2 mixture ( $x=0.67$ ) and by a further 7 °C for the 1:3 mixture ( $x=0.75$ ). At higher guest ratios, the  $\text{Col}_h$  phase is first strongly destabilized up to  $x=0.83$  (host/guest = 1:5), and eventually, a mixing gap is observed. This remarkable behavior can be explained by means of detailed X-ray studies and calculating the number of molecules per columnar unit (Table 1). All mixtures under investigation (**1/G1** = 1:1 (**1G1<sub>11</sub>**), 1:2 (**1G1<sub>12</sub>**), and 1:3 (**1G1<sub>13</sub>**)) show almost identical diffraction patterns at 93 °C. The cell parameters  $a$  of the  $\text{Col}_h$  phases amount to  $45.3 \pm 0.3$  Å, and the halos have the highest intensity at the meridian with an average hydrocarbon distance of 4.5 Å. Compared with the neat phase of dimers of **1**, the columnar diameters decrease slightly although the molecular masses of the hydrogen bond complexes increase. However, the columnar phases of the mixtures have to extend during the incorporation of the guest



molecules assuming a constant density of  $1 \text{ g cm}^{-3}$  of the LC phases. As the columnar diameters do not change significantly, the extension can only occur along the columnar axis. Starting from the dimer model, up to two guests per star mesogen can first be incorporated without a fundamental structural change of the columnar aggregates. The guests stabilize the columnar stacks by additional supramolecular interactions leading to an increase in the clearing temperatures of the mesophases. Upon integration of the guests, the columnar section  $c$ , which is filled by the dimer, increases from  $4.6 \text{ \AA}$  (**1**) to  $6.0 \text{ \AA}$  (**1G1<sub>12</sub>**; Table 1). Simultaneously, the amount of the 1:3 complex increases in the stoichiometric mixture for stochastic reasons (see the Supporting Information). These complexes cannot form dimers anymore and consequently destabilize the dimer phase incrementally (Figure 3). The cavities are completely filled in the mixture **1G1<sub>13</sub>**. Therefore, compound **1** has formed new supermesogens.<sup>[16]</sup> The new single building block, which assembles in a  $\text{Col}_h$  phase with a lower clearing temperature, but an identical columnar diameter compared to the dimer phase (Figure 4), fills a columnar section with a height of  $3.3 \text{ \AA}$  (Table 1). Owing to their structural similarity ( $\text{Col}_h$  phases, comparable columnar diameters  $a$ ), these phases are completely miscible. A model based on X-ray scattering results is shown in Figure 4D and E. The mesogens fit perfectly into the hexagonal cell. The aliphatic chains also project into the neighboring cells and fill the remaining free space. The

schematic representation clearly illustrates that the guests are enclosed by the host and neighboring supermesogens along the column. Thus, mesogen **1** can be denoted as a novel LC endoreceptor that is capable of hosting up to three guests. To fill the cavity, the hydrogen bonds are essential. Star mesogen **2** does not possess a hydrogen-bond acceptor that could compete with the hydrogen bonds of the cyclic dimers of the carboxylic acids **G1–G3**. Mixing studies with compound **2** and various adjusted guests did not generate stable mesophases (see the Supporting Information).

Aside from the transformation with guest **G1**, the formation of mesophases was investigated for the 1:3 mixtures of **1** with **G2** and **G3** (**1G2<sub>13</sub>** and **1G3<sub>13</sub>**), which possess more than one dodecyloxy chain. These mixtures also formed stable mesophases. The strong increase in the molecular mass of the supermesogens does not result in a larger columnar diameter, which is similar to the result with the mixture **1G1**. In contrast, the diameters even shrink slightly (Table 1). Therefore, the supermesogens can only stack along the column when the columns extend along their axes. The calculations in Table 1 demonstrate that the columnar section  $c$ , which is filled with one supermesogen at a density of  $1 \text{ g cm}^{-3}$ , increases from  $3.3 \text{ \AA}$  (**1G1<sub>13</sub>**) to  $3.9 \text{ \AA}$  (**1G2<sub>13</sub>**) and  $4.6 \text{ \AA}$  (**1G3<sub>13</sub>**). The clearing temperature decreases accordingly with an increase in the proportion of flexible chains.

The stabilities of the aggregates of **1** and the mixture **1G1<sub>13</sub>** were studied by X-ray scattering at the clearing temperature and in their isotropic phases. Moreover, the stability of the hydrogen bonds was investigated by temperature-dependent FT-IR spectroscopy. The X-ray studies confirm that the original correlation lengths, which can be calculated from the half width at half maximum by the Scherrer formula,<sup>[17]</sup> decrease from 32–53 columnar (molecular) diameters in the LC phases to 4–6 in the isotropic phases. Accordingly, the distance between the molecules decreases from 43–44  $\text{\AA}$  at  $129^\circ\text{C}$  to 32–36  $\text{\AA}$  in the isotropic phases, as the conformation of the chains in the molecules or aggregates is not restricted by the packing along the column anymore. In contrast to the dimer phase of **1**, the mixture **1G1<sub>13</sub>** shows a halo at small angles with a much higher intensity. Fitting the halos of the mixture reveals a second signal for the isotropic phases, which corresponds to a distance of 38  $\text{\AA}$  and can be attributed to the columnar phase (see the Supporting Information). This signal of the isotropic phase originates from a columnar aggregate with a correlation length of 8–9 columnar diameters. The relative intensity of these signals decreases with increasing temperature, but the signal still persists at  $215^\circ\text{C}$ . It is well known that after the clearing of a columnar phase, the columns do not completely disintegrate; therefore, the isotropic phase first consists of smaller columnar fragments.<sup>[18]</sup> Our findings thus confirm the higher stability of the columnar aggregates in the isotropic phase of the supermesogens **1G1<sub>13</sub>** compared to the columnar dimer aggregates of **1**. This may be attributed to the dissimilar shape and stability of the different columnar building blocks. Whereas the propeller-shaped dimers are interconnected by relatively weak dipolar interactions of the pyridyl units, the supermesogens generate a much more compact, planar, discotic structure, which is held together by strong hydrogen bonds. This assumption is

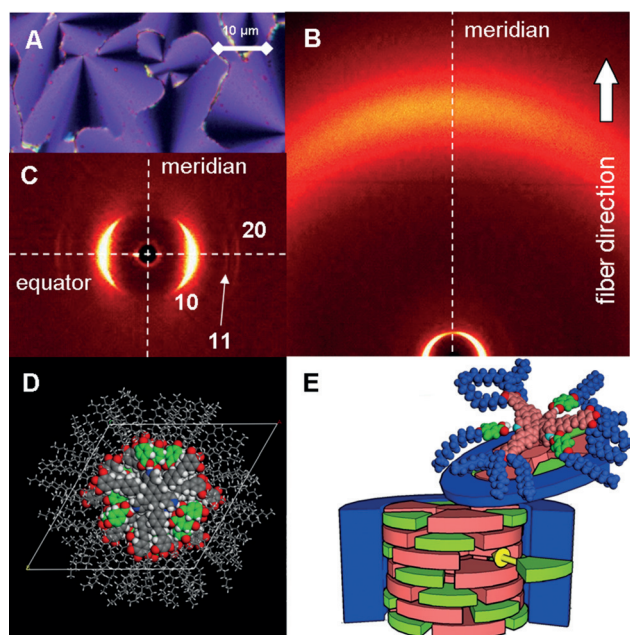


**Figure 4.** A) The pseudo-focal conic texture of **1G1<sub>13</sub>** at  $106^\circ\text{C}$  indicates a columnar phase. B) The WAXS diffraction pattern shows a halo with the highest intensity at the meridian. C) The reflections of the MAXS study at  $93^\circ\text{C}$  confirm the hexagonal symmetry. D, E) Model of the columnar phase of the supermesogen **1G1<sub>13</sub>**: Model based on a force-field geometry optimization (Compass, Materials Studio; D). The cores are displayed in space-filling, the chains in line representation. The bound guests are highlighted in green. E) Schematic representation of the supermesogen stacks. The guests (green) are completely enclosed; therefore, mesogen **1** can be considered as an endoreceptor.

supported by temperature-dependent FT-IR studies of **1G1<sub>3</sub>**. A broad band with a maximum at  $\tilde{\nu}=1680\text{ cm}^{-1}$  and shoulders at  $\tilde{\nu}=1700$  and  $1734\text{ cm}^{-1}$  demonstrates that in the equilibrium, various different hydrogen bonds ( $\tilde{\nu}=1680$ ,  $1700\text{ cm}^{-1}$ ) coexist with a tiny amount of free acid ( $\tilde{\nu}=1734\text{ cm}^{-1}$ ).<sup>[6]</sup> The amount of the latter increases from 5% at 90°C to only 9% in the isotropic phase just above the clearing temperature at 140°C. Even at 200°C, 50% of the hydrogen bonds are still intact (see the Supporting Information).

In conclusion, the demanding synthesis of new, shape-persistent, sterically crowded star mesogens has been achieved. The pyridyl derivative not only forms a novel dimer phase, for which the helical structure could be confirmed by X-ray scattering and simulation, but also serves as a threefold hydrogen-bond acceptor. It forms host-guest mesogens with various carboxylic acids, and the 1:3 mixtures reveal columnar phases of supermesogens with three guests. The guests are completely encompassed in the hexagonal phases; therefore, mesogen **1** can be considered as a new LC endoreceptor. This type of mesogens opens a new supramolecular access to highly organized LC materials. Adjusting the conjugated oligomer arms and the size of the cavities to selected functional guests will provide new LC materials in the future. Current studies involve derivatives with larger stilbenoid arms and chromophores as guest molecules.

**Keywords:** columnar phases · endoreceptors · hexasubstituted benzenes · liquid crystals · star mesogens

**How to cite:** *Angew. Chem. Int. Ed.* **2015**, *54*, 9710–9714  
*Angew. Chem.* **2015**, *127*, 9846–9850

- [1] C. Tschierske, *Angew. Chem. Int. Ed.* **2013**, *52*, 8828–8878; *Angew. Chem.* **2013**, *125*, 8992–9047.
- [2] M. Fritzsche, A. Bohle, D. Dudenko, U. Baumeister, D. Sebastiani, G. Richardt, H. W. Spiess, M. R. Hansen, S. Höger, *Angew. Chem. Int. Ed.* **2011**, *50*, 3030–3033; *Angew. Chem.* **2011**, *123*, 3086–3089.
- [3] M. Lehmann, *Star-shaped Mesogens in Handbook of Liquid Crystals*, Vol. 5, 2nd ed. (Eds.: J. W. Goodby, P. J. Collings, T. Kato, C. Tschierske, H. Gleeson, P. Raynes), Wiley-VCH, Weinheim, **2014**, Chapter 5.
- [4] M. Lehmann, M. Jahr, B. Donnio, R. Graf, S. Gemming, I. Popov, *Chem. Eur. J.* **2008**, *14*, 3562–3576.
- [5] a) M. Lehmann, M. Hügel, *Angew. Chem. Int. Ed.* **2015**, *54*, 4110–4114; *Angew. Chem.* **2015**, *127*, 4183–4187; b) M. Lehmann, B. Schartel, M. Hennecke, H. Meier, *Tetrahedron* **1999**, *55*, 13377–13394.
- [6] a) T. Kato, T. Yasuda, Y. Kamikawa, M. Yoshio, *Chem. Commun.* **2009**, 729–739; b) T. Kato, T. Uryu, F. Kaneuchi, C. Jin, J. M. J. Fréchet, *Liq. Cryst.* **1993**, *14*, 1311–1317.
- [7] a) J.-F. Xiong, S.-H. Luo, J.-P. Huo, J.-Y. Liu, S.-X. Chen, Z.-Y. Wang, *J. Org. Chem.* **2014**, *79*, 8366–8373; b) J. Barberá, L. Puig, P. Romero, J.-L. Serrano, T. Sierra, *J. Am. Chem. Soc.* **2006**, *128*, 4487–4492.
- [8] a) D. Janietz, *J. Mater. Chem.* **1998**, *8*, 265–274; b) D. Goldmann, D. Janietz, C. Schmidt, J. H. Wendorff, *J. Mater. Chem.* **2004**, *14*, 1521–1525; c) J. Barberá, L. Puig, J.-L. Serrano, T. Sierra, *Chem. Mater.* **2004**, *16*, 3308–3317; d) S. Coco, C. Cordovilla, C. Domínguez, B. Donnio, P. Espinet, D. Guillon, *Chem. Mater.* **2009**, *21*, 3282–3289.
- [9] H. Detert, M. Lehmann, H. Meier, *Materials* **2010**, *3*, 3218–3330.
- [10] Z. Tomović, J. van Dongen, S. J. George, H. Xu, W. Pisula, P. Leclère, M. M. Smulders, S. De Feyter, E. W. Meijer, A. P. Schenning, *J. Am. Chem. Soc.* **2007**, *129*, 16190–16196.
- [11] a) S. Ito, H. Inabe, N. Morita, K. Ohta, T. Kitamura, K. Imafuku, *J. Am. Chem. Soc.* **2003**, *125*, 1669–1680; b) S. Ito, M. Ando, A. Nomura, N. Morita, C. Kabuto, H. Mukai, K. Ohta, J. Kawakami, A. Yoshizawa, A. Tajiri, *J. Org. Chem.* **2005**, *70*, 3939–3949.
- [12] J. Nierle, D. Barth, D. Kuck, *Eur. J. Org. Chem.* **2004**, 867–872.
- [13] C. Knupp, J. M. Squire, *J. Appl. Crystallogr.* **2004**, *37*, 832–835.
- [14] O. Sumner Makin, P. Sikorski, L. C. Serpell, *J. Appl. Crystallogr.* **2007**, *40*, 966–972.
- [15] S. S. Sastry, T. V. Kumari, C. N. Rao, K. Mallika, S. Lakshminarayana, H. S. Tiong, *Adv. Cond. Matter Phys.* **2012**, 527065.
- [16] J. M. Lehn, *Supramolecular Chemistry - Concepts and Perspectives*. VCH, Weinheim, **1995**.
- [17] a) “Introduction to X-ray Powder Diffractometry”: R. Jenkins, R. L. Snyder, *Chemical Analysis*, Vol. 138, Wiley, New York, **1996**; b) P. Scherrer, *Nachr. Ges. Wiss. Göttingen, Math.-Phys. Kl.* **1918**, *2*, 98–100.
- [18] a) C. Krause, R. Zorn, F. Emmerling, J. Falkenhagen, B. Frick, P. Huber, A. Schönhals, *Phys. Chem. Chem. Phys.* **2014**, *16*, 7324–7333; b) W. K. Lee, P. A. Heiney, J. P. McCauley, A. B. Smith III, *Mol. Cryst. Liq. Cryst.* **1991**, *198*, 273–284; c) R. Kleppinger, C. P. Lillya, C. Yang, *J. Am. Chem. Soc.* **1997**, *119*, 4097–4102.

Received: March 3, 2015

Revised: April 17, 2015

Published online: June 23, 2015